ADVANCES IN ATMOSPHERIC SCIENCES, VOL. 39, APRIL 2022, 566–575

• News & Views •

The Nature and Predictability of the East Asian Extreme Cold Events of 2020/21※

Guokun DAI[1], Chunxiang LI[2], Zhe HAN*[2], Dehai LUO[2], and Yao YAO[2]

[1]*Department of Atmospheric and Oceanic Sciences and Institute of Atmospheric Sciences, Fudan University, Shanghai* 200438, *China*

[2]*CAS Key Laboratory of Regional Climate-Environment for Temperate East Asia, Institute of Atmospheric Physics, Chinese Academy of Sciences, Beijing* 100029, *China*

(Received 2 February 2021; revised 15 March 2021; accepted 31 March 2021)

ABSTRACT

Three extreme cold events invaded China during the early winter period between December 2020 to mid-January 2021 and caused drastic temperature drops, setting new low-temperature records at many stations during 6–8 January 2021. These cold events occurred under background conditions of low Arctic sea ice extent and a La Niña event. This is somewhat expected since the coupled effect of large Arctic sea ice loss in autumn and sea surface temperature cooling in the tropical Pacific usually favors cold event occurrences in Eurasia. Further diagnosis reveals that the first cold event is related to the southward movement of the polar vortex and the second one is related to a continent-wide ridge, while both the southward polar vortex and the Asian blocking are crucial for the third event. Here, we evaluate the forecast skill for these three events utilizing the operational forecasts from the ECMWF model. We find that the third event had the highest predictability since it achieves the best skill in forecasting the East Asian cooling among the three events. Therefore, the predictability of these cold events, as well as their relationships with the atmospheric initial conditions, Arctic sea ice, and La Niña deserve further investigation.

Key words: extreme cold event, predictability, Arctic atmospheric initial conditions, Arctic sea ice, La Niña

Citation: Dai, G. K., C. X. Li, Z. Han, D. H. Luo, and Y. Yao, 2022: The nature and predictability of the east asian extreme cold events of 2020/21. *Adv. Atmos. Sci.*, **39**(4), 566–575, https://doi.org/10.1007/s00376-021-1057-3.

1. Introduction

From mid-December 2020 to early January 2021, three strong surges of cold air swept through China, especially Eastern China. They occurred during 13–15, 29–31, December 2020, and 6–8 January 2021, and caused drastic and sudden temperature drops, with new low-temperature records set in Beijing City, Shandong, Hebei, and Shanxi Provinces. The area-averaged surface air temperature (SAT) anomalies over East Asia (20°–50°N, 100°–120°E) were two standard deviations below the daily climatology (Fig. 1a). Moreover, the mean SAT fell below the 10th percentile for the period 1979–2019 over widespread areas (Figs. 1b–d). Such severe cold events have significant impacts on public health, agriculture, infrastructure, transportation, and ecosystems and consequently have received broad attention.

Observations show that there was an increased frequency of extreme winter cold events which occurred in Eurasia during the past two decades (Cohen et al., 2014; 2020; Coumou and Rahmstorf, 2012; Johnson et al., 2018). For example, record-breaking low temperatures and severe blizzards affected many regions in East Asia during the 2010/11 winter (Gong et al., 2014). In January 2012, several cold surges invaded East Asia and two stations in Yunnan Province experienced record-breaking low daily temperatures. Moreover, southern China experienced an extended period of low temperatures, in addition to rain and snow events, during that period (Wu et al., 2017). In January 2016, a strong cold event affected East Asia and many stations set their low daily temperature records (Cheung et al., 2016; Song and Wu, 2017; Qian et al., 2018; Yamaguchi et al., 2019). During the winter of 2017/18, an extreme cold event occurred in East Asia, and record-breaking

※ This paper is a contribution to the special issue on Extreme Cold Events from East Asia to North America in Winter 2020/21.

* Corresponding author: Zhe HAN
Email: hanzhe@mail.iap.ac.cn

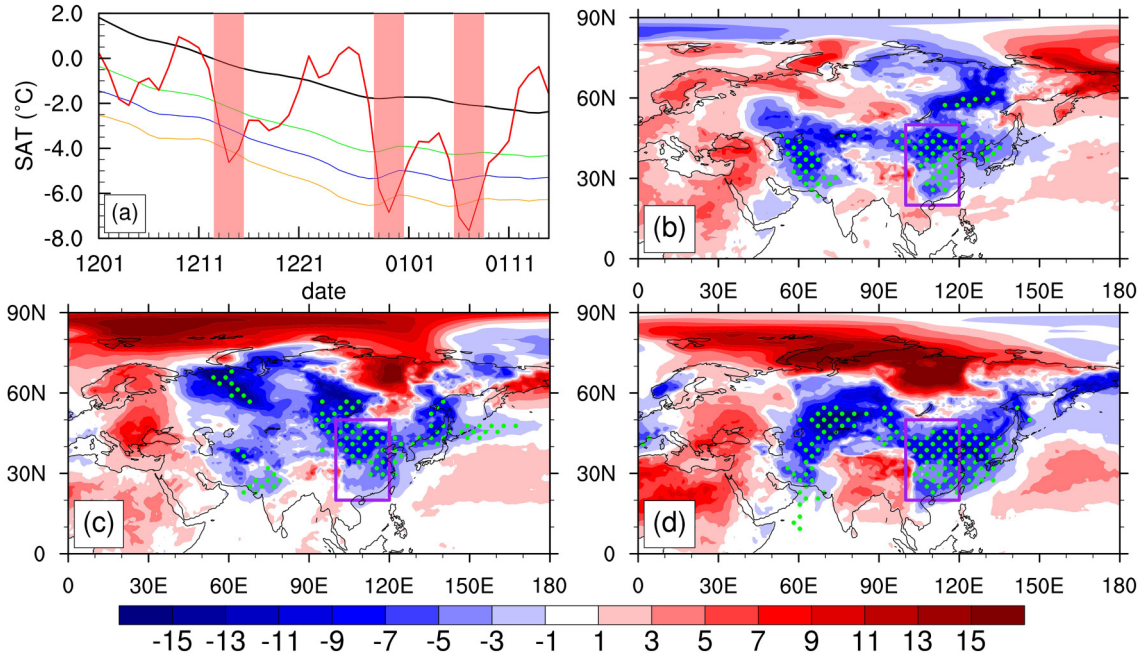

Fig. 1. (a) Time series of the SAT (units: °C) in East Asia (20°–50°N, 100°–120°E, red line) from 1 December 2020 to 15 January 2021, which is obtained from the ERA5 reanalysis. The *x*-axis is the date and the *y*-axis is the SAT in East Asia. The black line is the climatology, which is defined as the mean of 1979–2019. The green, blue, and orange lines represent −1.0, −1.5, and −2.0 standard deviations, respectively. The magenta shading indicates the extreme cold event periods. (b)–(d) are the mean SAT anomalies (shading, units: °C) during 13–15 December, 29–31 December 2020, and 6–8 January 2021, respectively. The dotted area indicates where the mean temperature fell below the 10th percentile during the 1979–2019 period. The purple boxes indicate the East Asia region (20°–50°N, 100°–120°E).

low temperatures were experienced over China, Japan, and Korea (Tachibana et al., 2019). The direct factor which triggered the extreme cold events is tied to a pattern of atmospheric circulation that favors the meridional transport of cold air from polar regions into East Asia which resulted in the drastic drops of SAT across the region. The atmospheric circulation pattern is usually related to blocking and the North Atlantic Oscillation, noting that these conditions are also modified by other factors, such as ENSO, the extent of Arctic sea ice, and Eurasian snow cover (Cheung et al., 2012; Park et al., 2014; Bollasina and Messori, 2018; Zhang et al., 2019; Li et al., 2021).

The increased frequency of extreme wintertime cold events in Eurasia seems to be related to the loss of Arctic sea ice (Wu et al., 2011a, b; Liu et al. 2012; Mori et al., 2014). It is probable that the globally-averaged meridional temperature gradient between the tropics and the Arctic has decreased due to Arctic sea ice loss, thus weakening the upper-tropospheric zonal wind component over the mid-latitudes in accordance with thermal wind balance. The weakened westerly momentum further leads to large amplitude waves within the jet streams and the associated slowly-propagating synoptic systems which are known to favor extreme event occurrences (Francis and Vavrus, 2012; Petoukhov et al., 2013; Screen and Simmonds, 2014). Moreover, some investigations pointed out that stratosphere–troposphere coupling is an essential pathway that links the loss of Arctic sea ice to the SAT cooling in Eurasia (Sun et al., 2015; Zhang et al., 2018). However, there are still many researchers who believe that the increase in extreme event occurrence is caused by the internal variability of the atmosphere, rather than the loss of Arctic sea ice since the linkage between the Arctic and Eurasia is poorly resolved by numerical models (McCusker et al., 2016; Blackport and Kushner, 2017; Ogawa et al., 2018; Blackport et al., 2019). However, observations show that the Arctic sea ice extent reached its second-lowest on record in September 2020, since 1979 (NASA, 2020), which, at least from a statistical perspective, appears to increase the likelihood of cold event occurrences in the following winter.

In addition to the low sea ice extent in the Arctic, the sea surface temperature in the tropical Pacific also plays an important role in modifying the frequency of Arctic air intrusions. As revealed by previous studies, the sea surface temperature cooling (warming) in the tropical Pacific favors the North Pacific anticyclone (cyclone) formation. Therefore, the East Asian winter monsoon is stronger (weaker) than usual in La Niña (El Niño) years, which appears to be favorable (unfavorable) to East Asian cold event occurrences (Wang et al., 2000; Chen, 2002; Sakai and Kawamura, 2009; He et al., 2013; Han et al., 2016; Zhang et al., 2019). The La Niña event which began in August 2020 soon developed into its mature phase, which, according to teleconnections, further supported the likelihood of extreme cold event occurrences during the 2020/21 winter

(CPC, 2021).

Both the Arctic sea ice and the sea surface temperature in the tropical Pacific provide favorable preconditions for the extreme cold event occurrences in the winter of 2020/21. However, these two factors alone cannot fully explain the extreme cold event occurrences.

2. Data and methods

The ERA5 reanalysis data that are used to identify the extreme cold events are obtained from the Copernicus Climate Data Store (https://cds.climate.copernicus.eu/#!/search?text=ERA5&type=dataset). The ERA5 reanalysis data are based on the Integrated Forecasting System release Cy41r2, which was operational in 2016, with a truncation of 639 waves in the horizontal (approximately 31 km) and 137 levels up to 0.01 hPa (around 80 km) in vertical. The ERA5 reanalysis data show an improved fit for temperature, wind, and humidity with radiosonde data in the troposphere, benefiting from a decade of developments in model physics, core dynamics, and 4D-Var data assimilation (Hersbach et al., 2020). The variables used in this investigation include the SAT, sea level pressure, and 500 hPa geopotential heightThe climatology is defined as the mean of a 5-day running average over the period 1979–2019 with a centered target date to remove the synoptic influence.

The daily operational forecast products from the ECMWF model are obtained from the International Grand Global Ensemble (TIGGE; Park et al., 2008; Swinbank et al., 2016) dataset, which is accessible through the ECMWF public data sets (https://apps.ecmwf.int/datasets/). The ECMWF numerical model is an atmosphere-ocean coupled system. The forecast products contain one control forecast and 50 perturbed forecasts with a forecast time of 15 days from each start time. The average of the 51 forecasts is defined as the ensemble mean forecast. The ERA5 climatology is used to calculate the forecast anomalies since the re-forecast data from the TIGGE dataset is not accessible.

The sub-seasonal to seasonal (S2S; Vitart et al., 2017) forecasts in the ECMWF are carried out twice per week (each Monday and Thursday) with an integration of 46 days, which can be downloaded from the ECMWF public data sets (https://apps.ecmwf.int/datasets/). The S2S forecasts include 51 real-time ensemble forecasts and 220 re-forecasts. The 51 real-time ensemble forecasts contain one control forecast and 50 perturbed forecasts, which are similar to those in TIGGE dataset. The re-forecasts in ECMWF are conducted on the fly to ensure the model consistency between the real-time forecasts and re-forecasts. The on the fly re-forecasts have 11 ensemble members (one control re-forecast and 10 perturbed members) for the past 20 years. Therefore, the mean of the 20 control re-forecasts is defined as the model climatology for the real-time control forecasts while the mean of the 220 ensemble re-forecasts is reserved for the real-time ensemble mean forecasts.

3. Overview of three cold events

There were three extreme cold events between 1 December 2020 and 15 January 2021. The cold outbreaks occurred within a synoptic environment that featured an intensified Siberian High and deepened Aleutian Low. This pattern resulted in strong northerly flow along the east coast of China which ultimately led to a drastic SAT drop in East Asia. However, the atmospheric circulations related to the three extreme cold events are not identical.

The first cold event occurred during 13–15 December 2020. Compared to the climatological circulation in December and January (Fig. 2a), the polar vortex was weaker than normal and the East Asian Trough was deeper than normal at 500 hPa (Fig. 2b). In terms of sea level pressure, both the Siberian High and Aleutian Low were stronger than normal, thereby increasing the northeasterly winds over East Asia. This pattern led to rapid temperature drops and an ensuing cold air outbreak over East Asia which propagated from north to south over the course of two days. This particular cold event was mainly related to the southward displacement of the polar vortex. Therefore, this event was also accompanied by cooling SAT in the Arctic and northern Siberia although there was some warming to the west of Lake Baikal due to a geopotential height ridge near the Aral Sea.

The second event, which occurred during 29–31 December 2020, featured the patterns of SLP and geopotential height at 500 hPa that are shown in Fig. 2c. There was a continent-wide ridge over Eurasia with two centers, one over the Barents Sea and the other one over northern Siberia. The extended ridge embedded itself into polar regions, leading to a weak polar vortex. Along with the geopotential height center over northern Siberia, the Siberian High strengthened to the northwest of Lake Baikal, with an intensity greater than 1050 hPa. Moreover, the East Asian Trough deepened and this combination resulted in the strong northerly transport of a cold air mass from the Arctic into East Asia. Therefore, the SAT in East Asia suddenly dropped during that period. Meanwhile, there was a drastic and commensurate SAT warming in the Arctic, thereby establishing a warm Arctic-cold Eurasia pattern.

Figure 2d shows the SLP and geopotential height at 500 hPa for the third cold event during 6–8 January 2021. During the pause between the second and third cold event, the continent-wide ridge over Eurasia was strengthened by a blocking event to the west of Lake Baikal which split the polar vortex. The blocking pattern to the west of Lake Baikal exhibited a

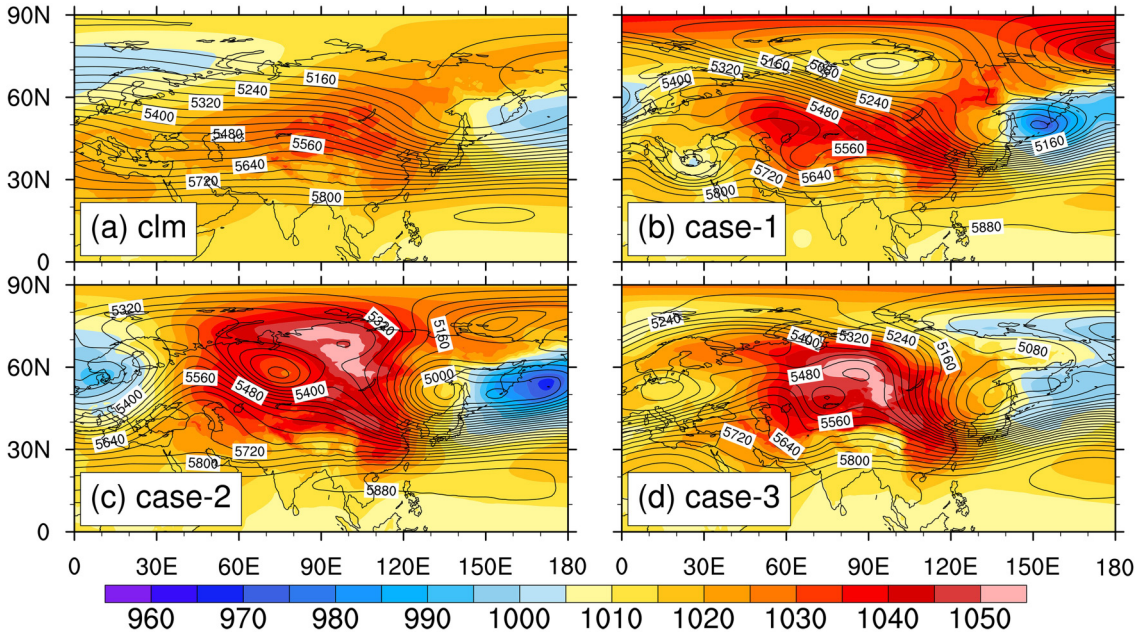

Fig. 2. The mean sea level pressure (shading, units: hPa) and geopotential height (contour, units: gpm, contour interval CI = 40 gpm) at 500 hPa. (a) is for the climatology in December and January during 1979–2019. (b)–(d) correspond to the three cold events, which occurred on 13–15 December 2020, 29–31 December 2020, and 6–8 January 2021, respectively.

northeast-southwest dipole structure, which supported north winds transporting cold air into East Asia (Luo et al., 2016). Along with the blocking, the Siberian High strengthened and moved southward, with an intensity greater than 1050 hPa. Moreover, the southeastward moving split polar vortex deepened the East Asian Trough and transported the cold air from eastern Siberia to East Asia, which further exacerbated the cooling in East Asia. Therefore, many stations in East Asia experienced record-breaking low temperatures during this period.

It seems that the mean atmospheric circulation anomalies of the last two events have similar characteristics. Yet, from their daily evolutions, it is obvious to see that the second event was caused by a transverse trough which changed its orientation to vertical, which is related to the development of the continent-wide ridge (Fig. A1 in the Appendix). However, the trigger for the last event was the southward movement of the East Asian cyclone, which was forced by both the Asian blocking and the southward displacement of the polar vortex (Fig. A2). Therefore, the first cold event is related to the southward movement of the polar vortex and the second one is related to the continent-wide ridge. But for the third event, both the southward displacement of the polar vortex and the Asian blocking were important.

4. Forecast skill for the events

It is important to skillfully forecast these extreme cold events due to their great economic and social effects. Utilizing the operational forecast products from the ECMWF model, forecast performances of the East Asian SAT for the three extreme cold events with a lead time of five days are shown in Figs. 3a–c. We find that the ensemble mean can capture the East Asian cooling during these periods, however, the first cold event was underestimated (Fig. 3a). Moreover, almost all the ensemble members forecasted the East Asian cooling to be stronger than −2.0 standard deviations for the third event, while most of the ensemble members forecasted the cooling stronger than −1.0 (−1.5) standard deviations for the first (second) event.

In addition to the mean SAT, the forecasts from ECMWF also have captured the general circulation patterns and the spatial distribution of the cooling in East Asia. However, the control forecast, which started on 8 December, underestimates the strength of the polar vortex over northern Siberia and the depth of the East Asian Trough during 13–15 December but demonstrates the SAT anomaly well during that period (Fig. 4a). For the second cold event occurring during 29–31 December, the control forecast started on 24 December was able to reproduce the continent-wide ridge over Eurasia well, although the positions of the two centers in the control forecast are somewhat different from those in reanalysis (Fig. 4b). With regard to the third cold event, the control forecast started on 1 January 2021 was able to reproduce the continent-wide ridge over Eurasia and the deepened East Asian Trough despite the forecasted Asian blocking being positioned further to the northeast than in the reanalysis (Fig. 4c). Therefore, the cooling in East Asia was well forecasted. In addition to the control forecasts, the

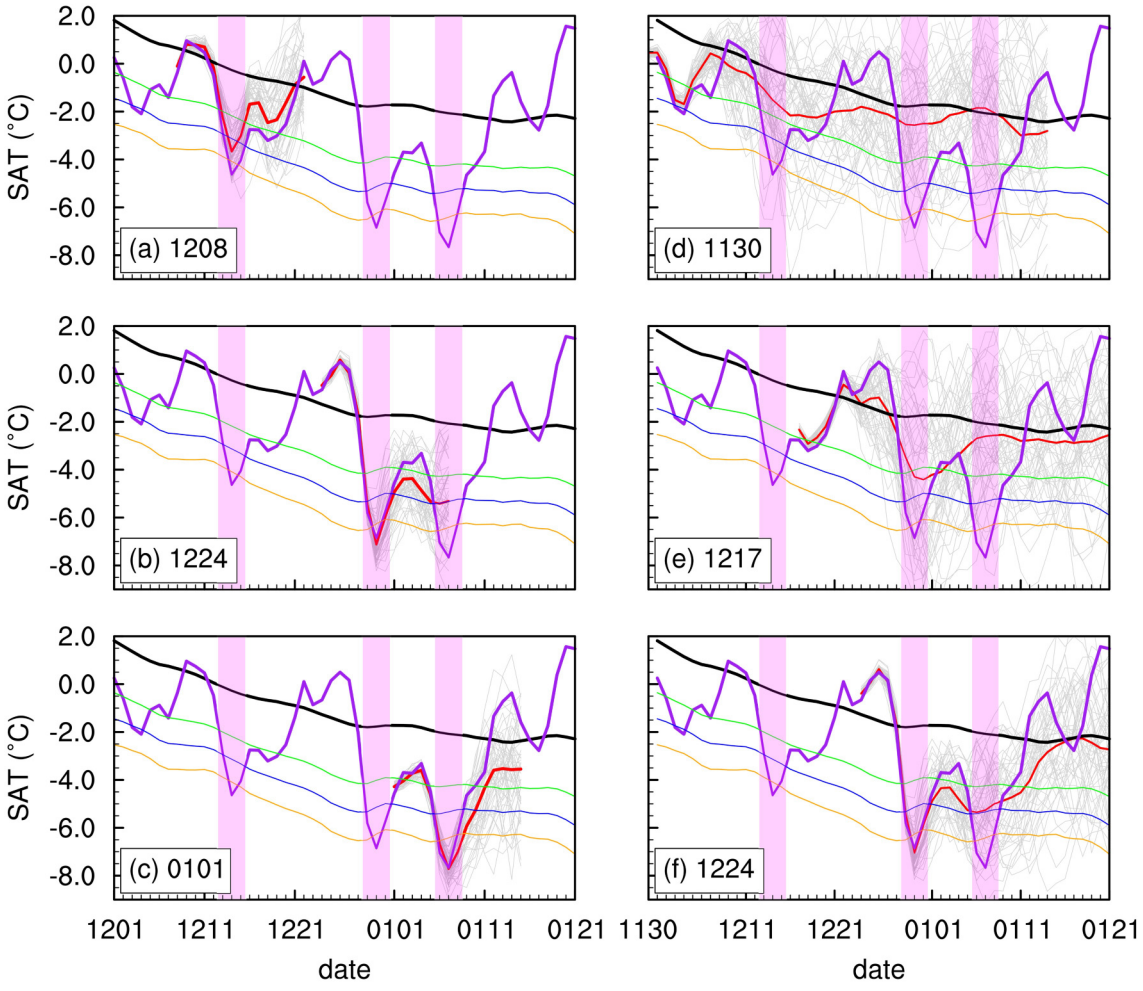

Fig. 3. The forecast average SAT (units: °C) in East Asia for the three cold events. The *x*-axis is the date and the *y*-axis is the SAT in East Asia. The black line is the climatology, which is defined as the mean of 1979–2019. The green, blue, and orange lines represent −1.0, −1.5, and −2.0 standard deviations, respectively. The magenta shading indicates the extreme cold event periods. The purple line is the observed SAT in East Asia, which is derived from ERA5 reanalysis data. Fifty-one gray lines in each panel indicate the 51 ensemble forecast members and the red line is the ensemble mean. (a)–(c) are derived from TIGGE data, with a forecast lead time of 5 days, while (d)–(f) are derived from S2S data, with a forecast lead time of 12 or 13 days. (a) and (d) are for case 1, (b) and (e) for case 2, and (c) and (f) are for case 3.

ensemble mean forecasts for the three cold events are shown as Figs. 4d–f. They show similar SAT anomalies and geopotential height patterns for their corresponding control forecasts, but with a relatively weaker intensity.

Additionally, previous studies suggest that some extreme cold events could be skillfully forecasted with lead times longer than two weeks (Dai and Mu, 2020a; Dai et al., 2021). Whether these extreme cold events can be forecasted with a lead time longer than two weeks deserves further investigation. Utilizing the S2S forecast products from ECMWF, the mean SAT forecasts in East Asia for the three extreme cold events with a lead time of 12 or 13 days are shown in Figs. 3d–f. The cooling during these cold event periods was underestimated by the ensemble mean. Specifically, the ensemble mean forecast of East Asian cooling is weaker than −1.0 standard deviations for the first event (Fig. 3d), around −1.0 standard deviations for the second event, and −1.5 standard deviations for the last event (Figs. 3e–f). This indicates that the forecast skill of the last cold event was best among the three events, with a forecast lead time longer than 10 days.

Moreover, the sub-seasonal forecasts of the SAT anomaly and geopotential height at 500 hPa for these three cold events are further investigated (Fig. 5). The first cold event was accompanied by a southwardly displaced polar vortex over north Siberia in the control forecast which started on 30 November. However, the polar vortex in the control forecast does not reach as far south as that in reanalysis. Therefore, the most dramatic cooling in the control forecast is located to the north of that in reanalysis (Fig. 5a). In the ensemble mean forecast, both the polar vortex and associated cooling have consistent locations with those in reanalysis, but with a weaker intensity (Fig. 5d). However, for the second extreme cold event, the strong northerly flow near Lake Baikal is well-described and the SAT cooling in East Asia is captured in the control fore-

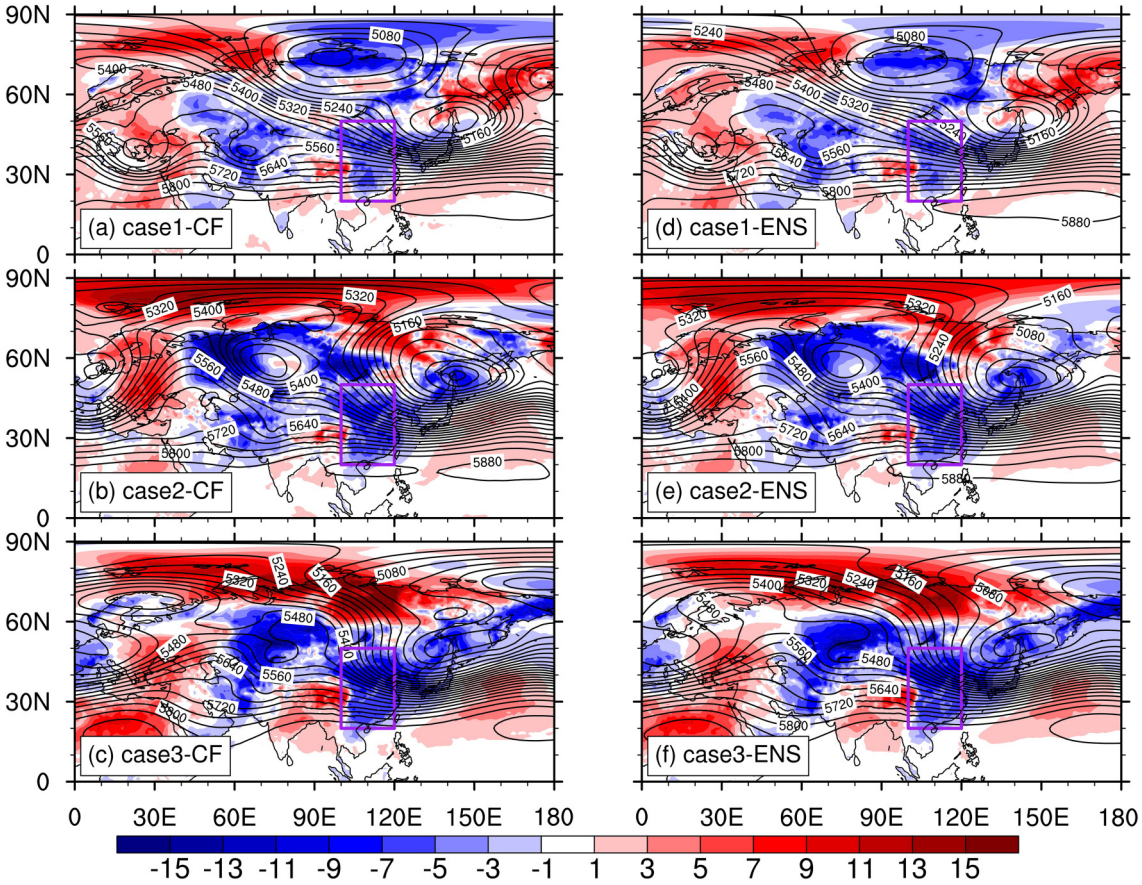

Fig. 4. The forecast SAT anomaly (shading, units: °C) and geopotential height (contour, units: gpm, CI = 40 gpm) at 500 hPa for the cold event periods, with a forecast lead time of five days. (a) and (d) are the mean of 13–15 December 2020 derived from the forecasts started on 8 December 2020, (b) and (e) are the mean of 29–31 December 2020 derived from the forecasts started on 24 December 2020, while (c) and (f) are the mean of 6–8 January 2021 derived from the forecasts started on 1 January 2021. (a)–(c) are derived from the control forecasts while (d)–(f) correspond to the ensemble mean. The purple boxes indicate the East Asia region (20°–50°N, 100°–120°E).

cast started on 17 December, however, the continent-wide ridge is different in spatial character from that in the reanalysis (Fig. 5b). The third extreme cold event is captured in the control forecast started on 24 December (Fig. 5c). Both the continent-wide ridge over Eurasia and the deepened East Asian Trough are well described, although the Asian blocking event is missing. In addition to the control forecasts, the ensemble mean forecasts have similar patterns with their respective control forecasts, for both the geopotential height and SAT anomalies, but with weaker intensities (Figs. 5e–f). We may conclude that the third cold event was forecasted best among the three cases.

5. Discussions

For medium-range and sub-seasonal timescales, the atmospheric initial conditions play an important role in determining the skill of extreme cold event forecasts. However, the Arctic is a region characterized by large atmospheric uncertainties due to the sparseness of observations (Inoue et al., 2011; Jung et al., 2014). Previous studies suggest that the medium-range and extended-range forecasts of 500 hPa geopotential height in the Northern Hemisphere can be improved with a more accurate initial representation of the Arctic atmosphere (Jung et al., 2014). Recently, Dai and Mu (2020b) investigated a cold surge that occurred in East Asia during 21–25 January 2016 and found that the skill of 10-day weather forecast is sensitive to the atmospheric initial conditions in the Arctic. A possible reason for this concerns the northerly winds which lead to a cold surge, which act to underscore the influence of the upstream Arctic atmosphere (Semmler et al., 2018). However, the forecast skill is not always improved when more observations in the Arctic are used (Sato et al., 2017).

In addition to the atmospheric initial conditions, boundary conditions such as sea ice and sea surface temperature anomalies may also influence the predictability of East Asian extreme cold events. Boundary conditions are known to be crucial for sub-seasonal forecasts and may consequently contribute to the predictability of extreme cold events (Deser et al., 2007; Semmler et al., 2016). However, such studies are few and the physical mechanisms that explain their roles in supporting the

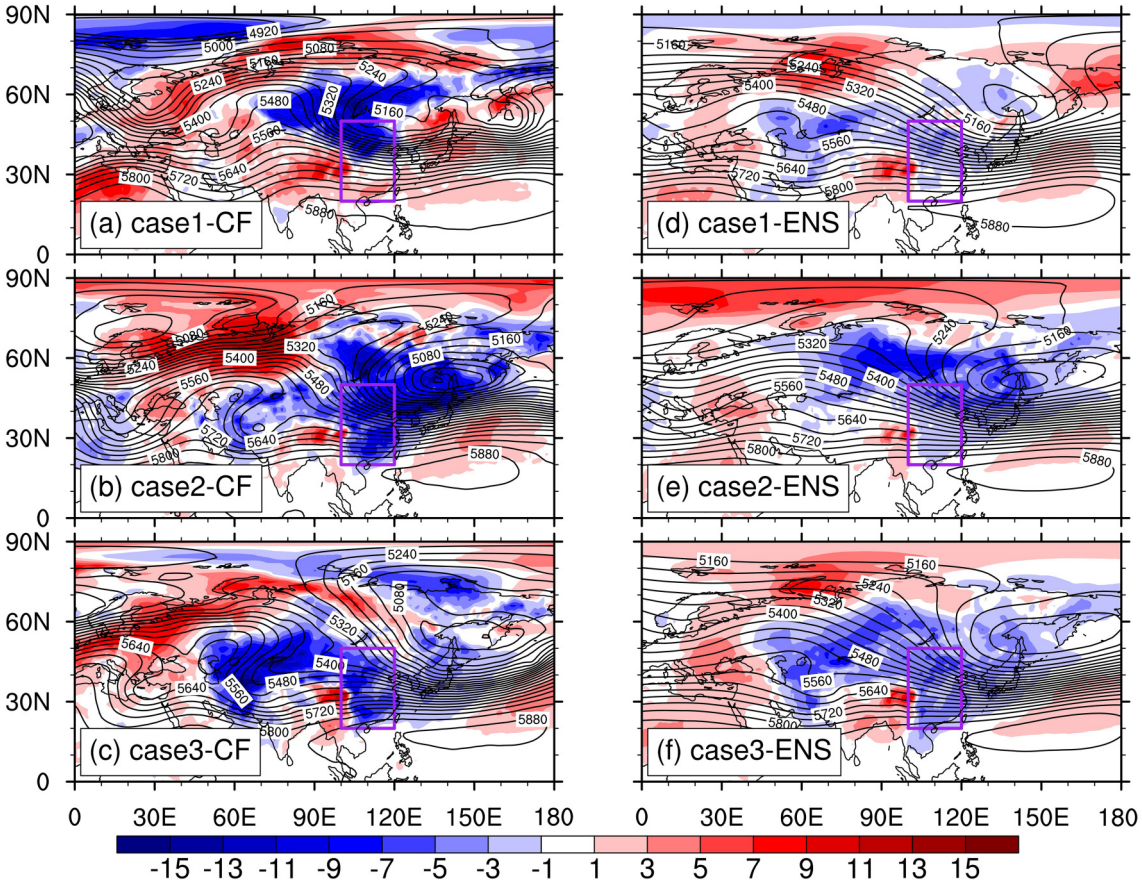

Fig. 5. The forecast SAT anomaly (shading, units: °C) and geopotential height (contour, units: gpm, CI = 40 gpm) at 500 hPa for the cold event periods, with a forecast lead time of 12 or 13 days. (a) and (d) are the mean of 13–15 December 2020 derived from the forecasts started on 30 November 2020, (b) and (e) are the mean of 29–31 December 2020 derived from the forecasts started on 17 December 2020, while (c) and (f) are the mean of 6–8 January 2021 derived from the forecasts started on 24 December 2020. (a)–(c) are derived from the control forecasts while (d)–(f) correspond to the ensemble mean. The purple boxes indicate the East Asia region (20°–50°N, 100°–120°E).

cold events on sub-seasonal timescales are not clear.

Among the three extreme cold events in 2020/21, the forecast skill for the first two cold events is lower than the third one. Why are the forecast skills different for these events? What is the role played by the Arctic atmospheric initial conditions? Moreover, studies show that the stratosphere is an essential source of predictability for extreme cold events (Cai et al., 2016; Yu et al., 2018). Do stratospheric processes contribute to triggering these cold events? These topics are worthy of further investigation.

Acknowledgements. The authors acknowledge the support from the National Natural Science Foundation of China (Grant Nos: 41790475, 42005046, and 41790473) and three anonymous reviewers for their helpful comments in improving this paper.

APPENDIX

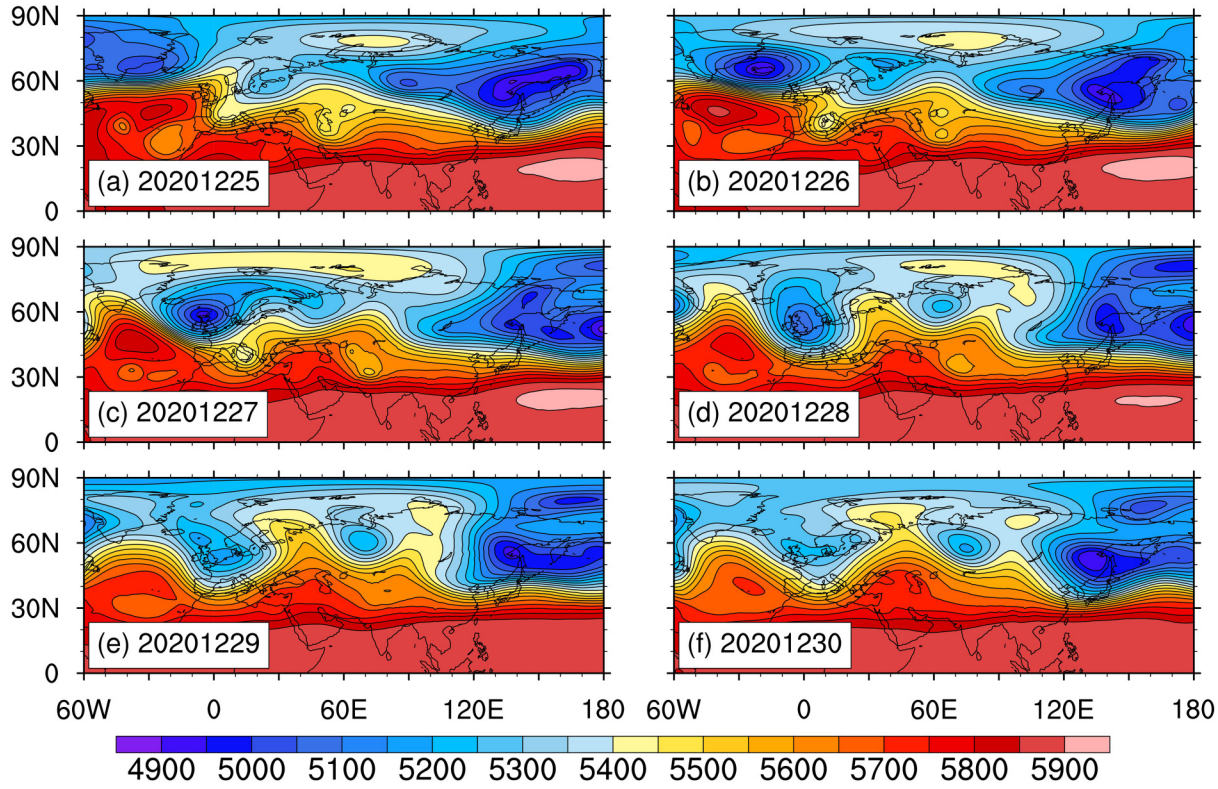

Fig. A1. The daily geopotential height (units: gpm) at 500 hPa from 25 to 30 December 2020, which are derived from ERA5 reanalysis data.

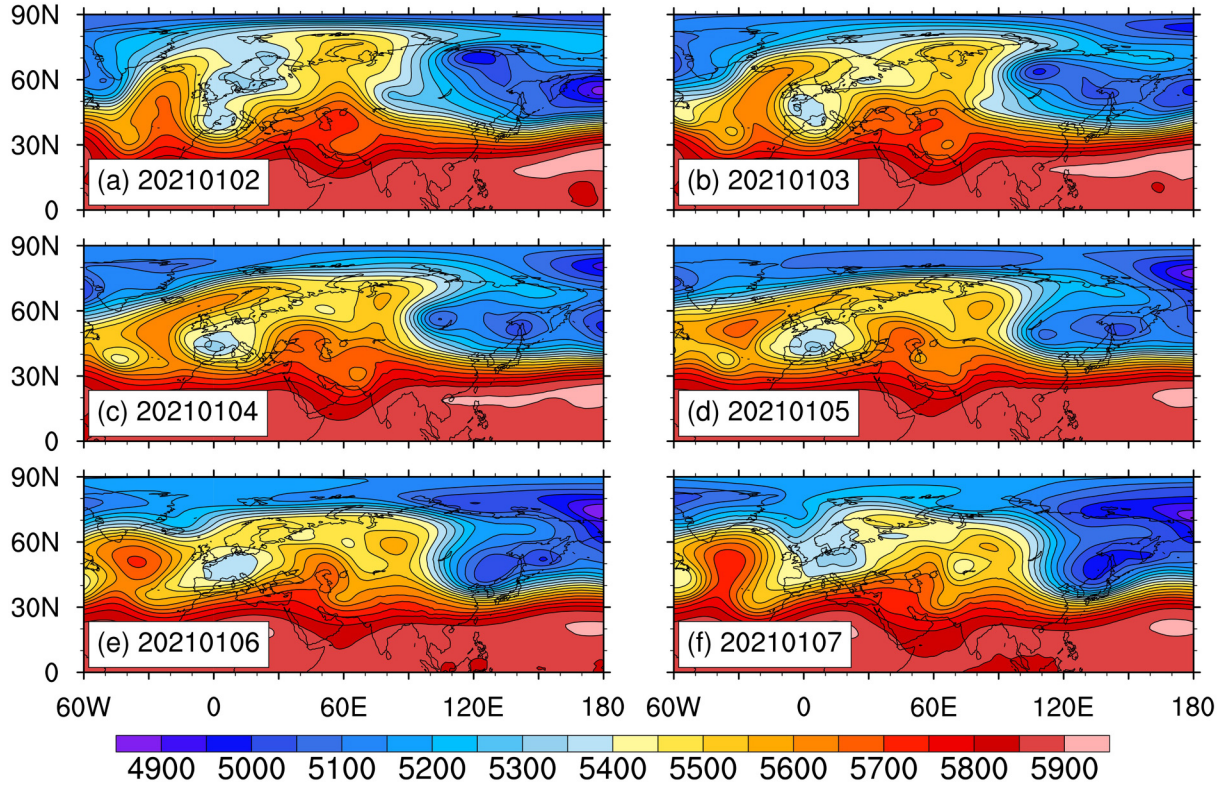

Fig. A2. As in Fig. A1, but for the period from 2 to 7 January 2021.

REFERENCES

Blackport, R., and P. J. Kushner, 2017: Isolating the atmospheric circulation response to arctic sea ice loss in the coupled climate system. *J. Climate*, **30**(6), 2163–2185, https://doi.org/10.1175/JCLI-D-16-0257.1.

Blackport, R., J. A. Screen, K. van der Wiel, and R. Bintanja, 2019: Minimal influence of reduced Arctic sea ice on coincident cold winters in mid-latitudes. *Nature Climate Change*, **9**, 697–704, https://doi.org/10.1038/s41558-019-0551-4.

Bollasina, M. A., and G. Messori, 2018: On the link between the subseasonal evolution of the North Atlantic Oscillation and East Asian climate. *Climate Dyn.*, **51**, 3537–3557, https://doi.org/10.1007/S00382-018-4095-5.

Cai, M., Y. Y. Yu, Y. Deng, H. M. van den Dool, R. C. Ren, S. Saha, X. R. Wu, and J. Huang, 2016: Feeling the pulse of the stratosphere: An emerging opportunity for predicting continental-scale cold-air outbreaks 1 month in advance. *Bull. Amer. Meteor. Soc.*, **97**(8), 1475–1489, https://doi.org/10.1175/BAMS-D-14-00287.1.

Chen, W., 2002: Impacts of El Niño and La Niña on the cycle of the East Asian winter and summer monsoon. *Chinese Journal of Atmospheric Sciences*, **26**, 595–610, https://doi.org/10.3878/j.issn.1006-9895.2002.05.02. (in Chinese with English abstract)

Cheung, H. H. N., W. Zhou, M. Y. T. Leung, C. M. Shun, S. M. Lee, and H. W. Tong, 2016: A strong phase reversal of the Arctic Oscillation in midwinter 2015/2016: Role of the stratospheric polar vortex and tropospheric blocking. *J. Geophys. Res.*, **121**(22), 13 443–13 457, https://doi.org/10.1002/2016JD025288.

Cheung, H. N., W. Zhou, H. Y. Mok, and M. C. Wu, 2012: Relationship between Ural-Siberian blocking and the East Asian winter monsoon in relation to the Arctic Oscillation and the El Niño-Southern Oscillation. *J. Climate*, **25**(12), 4242–4257, https://doi.org/10.1175/JCLI-D-11-00225.1.

Cohen, J., and Coauthors, 2014: Recent Arctic amplification and extreme mid-latitude weather. *Nature Geoscience*, **7**(9), 627–637, https://doi.org/10.1038/ngeo2234.

Cohen, J., and Coauthors, 2020: Divergent consensuses on Arctic amplification influence on midlatitude severe winter weather. *Nature Climate Change*, **10**(1), 20–29, https://doi.org/10.1038/s41558-019-0662-y.

Coumou, D., and S. Rahmstorf, 2012: A decade of weather extremes. *Nature Climate Change*, **2**(7), 491–496, https://doi.org/10.1038/nclimate1452.

CPC, 2021: El Niño/Southern Oscillation (ENSO) diagnostic discussion. Available from https://www.cpc.ncep.noaa.gov/products/analysis_monitoring/enso_advisory/ensodisc.shtml.

Dai, G. K., and M. Mu, 2020a: Influence of the Arctic on the predictability of Eurasian winter extreme weather events. *Adv. Atmos. Sci.*, **37**(4), 307–317, https://doi.org/10.1007/s00376-019-9222-7.

Dai, G. K., and M. Mu, 2020b: Arctic influence on the Eastern Asian Cold Surge Forecast: A case study of January 2016. *J. Geophys. Res.*, **125**(23), e2020JD033298, https://doi.org/10.1029/2020JD033298.

Dai, G. K., M. Mu, C. X. Li, Z. Han, and L. Wang, 2021: Evaluation of the forecast performance for extreme cold events in East Asia with subseasonal-to-seasonal data sets from ECMWF. *J. Geophys. Res.*, **126**, 2020JD033860, https://doi.org/10.1029/2020JD033860.

Deser, C., R. A. Tomas, and S. L. Peng, 2007: The transient atmospheric circulation response to North Atlantic SST and sea ice anomalies. *J. Climate*, **20**(18), 4751–4767, https://doi.org/10.1175/JCLI4278.1.

Francis, J. A., and S. J. Vavrus, 2012: Evidence linking Arctic amplification to extreme weather in mid-latitudes. *Geophys. Res. Lett.*, **39**, L06801, https://doi.org/10.1029/2012GL051000.

Gong, Z. Q., G. L. Feng, F. M. Ren, and J. P. Li, 2014: A regional extreme low temperature event and its main atmospheric contributing factors. *Theor. Appl. Climatol.*, **117**(1), 195–206, https://doi.org/10.1007/S00704-013-0997-7.

Han, Z., S. L. Li, J. P. Liu, Y. Q. Gao, and P. Zhao, 2016: Linear additive impacts of arctic sea ice reduction and La Nina on the northern hemisphere winter climate. *J. Climate*, **29**, 5513–5532, https://doi.org/10.1175/JCLI-D-15-0416.1.

He, S. P., H. J. Wang, and J. P. Liu, 2013: Changes in the relationship between ENSO and Asia-Pacific midlatitude winter atmospheric circulation. *J. Climate*, **26**, 3377–3393, https://doi.org/10.1175/JCLI-D-12-00355.1.

Hersbach, H., and Coauthors, 2020: The ERA5 global reanalysis. *Quart. J. Roy. Meteor. Soc.*, **146**(730), 1999–2049, https://doi.org/10.1002/qj.3803.

Inoue, J., M. E. Hori, T. Enomoto, and T. Kikuchi, 2011: Intercomparison of surface heat transfer near the Arctic marginal ice zone for multiple reanalyses: A case study of September 2009. *SOLA*, **7**, 57–60, https://doi.org/10.2151/SOLA.2011-015.

Johnson, N. C., S.-P. Xie, Y. Kosaka, and X. C. Li, 2018: Increasing occurrence of cold and warm extremes during the recent global warming slowdown. *Nature Communications*, **9**(1), 1724, https://doi.org/10.1038/s41467-018-04040-y.

Jung, T., M. A. Kasper, T. Semmler, and S. Serrar, 2014: Arctic influence on subseasonal midlatitude prediction. *Geophys. Res. Lett.*, **41**, 3676–3680, https://doi.org/10.1002/2014GL059961.

Li, M. Y., D. H. Luo, I. Simmonds, A. G. Dai, L. H. Zhong, and Y. Yao, 2021: Anchoring of atmospheric teleconnection patterns by Arctic sea ice loss and its link to winter cold anomalies in East Asia. *International Journal of Climatology*, **41**(1), 547–558, https://doi.org/10.1002/joc.6637.

Liu, J. P., J. A. Curry, H. J. Wang, M. R. Song, and R. M. Horton, 2012: Impact of declining Arctic sea ice on winter snowfall. *Proceedings of the National Academy of Sciences of the United States of America*, **109**, 4074–4079, https://doi.org/10.1073/pnas.1114910109.

Luo, D. H., Y. Q. Xiao, Y. N. Diao, A. G. Dai, C. L. E. Franzke, and I. Simmonds, 2016: Impact of Ural blocking on winter warm Arctic–cold Eurasian anomalies. Part II: The link to the North Atlantic Oscillation. *J. Climate*, **29**(11), 3949–3971, https://doi.org/10.1175/JCLI-D-15-0612.1.

McCusker, K. E., J. C. Fyfe, and M. Sigmond, 2016: Twenty-five winters of unexpected Eurasian cooling unlikely due to Arctic sea-ice

loss. *Nature Geoscience*, **9**(11), 838–842, https://doi.org/10.1038/ngeo2820.
Mori, M., M. Watanabe, H. Shiogama, J. Inoue, and M. Kimoto, 2014: Robust Arctic sea-ice influence on the frequent Eurasian cold winters in past decades. *Nature Geoscience*, **7**, 869–873, https://doi.org/10.1038/ngeo2277.
NASA, 2020: 2020 arctic sea ice minimum at second lowest on record. Available from https://www.nasa.gov/feature/goddard/2020/2020-arctic-sea-ice-minimum-at-second-lowest-on-record/.
Ogawa, F., and Coauthors, 2018: Evaluating impacts of recent arctic sea ice loss on the Northern Hemisphere winter climate change. *Geophys. Res. Lett.*, **45**(7), 3255–3263, https://doi.org/10.1002/2017GL076502.
Park, T. W., C. H. Ho, and Y. Deng, 2014: A synoptic and dynamical characterization of wave-train and blocking cold surge over East Asia. *Climate Dyn.*, **43**(3–4), 753–770, https://doi.org/10.1007/s00382-013-1817-6.
Park, Y. Y., R. Buizza, and M. Leutbecher, 2008: TIGGE: Preliminary results on comparing and combining ensembles. *Quart. J. Roy. Meteor. Soc.*, **134**(637), 2029–2050, https://doi.org/10.1002/qj.334.
Petoukhov, V., S. Rahmstorf, S. Petri, and H. J. Schellnhuber, 2013: Quasiresonant amplification of planetary waves and recent Northern Hemisphere weather extremes. *Proceedings of the National Academy of Sciences of the United States of America*, **110**(14), 5336–5341, https://doi.org/10.1073/pnas.1222000110.
Qian, C., and Coauthors, 2018: Human influence on the record-breaking cold event in January of 2016 in Eastern China. *Bull. Amer. Meteor. Soc*, **99**(1), S118–S122, https://doi.org/10.1175/BAMS-D-17-0095.1.
Sakai, K., and R. Kawamura, 2009: Remote response of the East Asian winter monsoon to tropical forcing related to El Niño-Southern Oscillation. *J. Geophys. Res.*, **114**(D6), D06105, https://doi.org/10.1029/2008jd010824.
Sato, K., J. Inoue, A. Yamazaki, J.-H. Kim, M. Maturilli, K. Dethloff, S. R. Hudson, and M. A. Granskog, 2017: Improved forecasts of winter weather extremes over midlatitudes with extra Arctic observations. *J. Geophys. Res.*, **122**, 775–787, https://doi.org/10.1002/2016JC012197.
Screen, J. A., and I. Simmonds, 2014: Amplified mid-latitude planetary waves favour particular regional weather extremes. *Nature Climate Change*, **4**(8), 704–709, https://doi.org/10.1038/nclimate2271.
Semmler, T., T. Jung, and S. Serrar, 2016: Fast atmospheric response to a sudden thinning of Arctic sea ice. *Climate Dyn.*, **46**(3-4), 1015–1025, https://doi.org/10.1007/s00382-015-2629-7.
Semmler, T., T. Jung, M. Kasper, and S. Serrar, 2018: Using NWP to assess the influence of the Arctic atmosphere on midlatitude weather and climate. *Adv. Atmos. Sci.*, **35**(1), 5–13, https://doi.org/10.1007/s00376-017-6290-4.
Song, L., and R. G. Wu, 2017: Processes for occurrence of strong cold events over eastern China. *J. Climate*, **30**(22), 9247–9266, https://doi.org/10.1175/JCLI-D-16-0857.1.
Sun, L. T., C. Deser, and R. A. Tomas, 2015: Mechanisms of stratospheric and tropospheric circulation response to projected arctic sea ice loss. *J. Climate*, **28**(19), 7824–7845, https://doi.org/10.1175/JCLI-D-15-0169.1.
Swinbank, R., and Coauthors, 2016: The TIGGE project and its achievements. *Bull. Amer. Meteor. Soc.*, **97**(1), 49–67, https://doi.org/10.1175/BAMS-D-13-00191.1.
Tachibana, Y., K. K. Komatsu, V. A. Alexeev, L. Cai, and Y. Ando, 2019: Warm hole in Pacific Arctic sea ice cover forced mid-latitude Northern Hemisphere cooling during winter 2017–18. *Scientific Reports*, **9**(1), 5567, https://doi.org/10.1038/S41598-019-41682-4.
Vitart, F., and Coauthors, 2017: The Subseasonal to seasonal (S2S) prediction project database. *Bull. Amer. Meteor. Soc.*, **98**(1), 163–173, https://doi.org/10.1175/BAMS-D-16-0017.1.
Wang, B., R. G. Wu, and X. H. Fu, 2000: Pacific-East Asian teleconnection: How does ENSO affect East Asian climate? *J. Climate*, **13**, 1517–1536, https://doi.org/10.1175/1520-0442(2000)013<1517:PEATHD>2.0.CO;2.
Wu, B. Y., J. Z. Su, and R. H. Zhang, 2011a: Effects of autumn-winter Arctic sea ice on winter Siberian high. *Chinese Science Bulletin*, **56**, 3220–3228, https://doi.org/10.1007/s11434-011-4696-4.
Wu, B. Y., K. Yang, and J. A. Franci, 2017: A cold event in Asia during January-February 2012 and its possible association with Arctic sea ice loss. *J. Climate*, **30**(19), 7971–7990, https://doi.org/10.1175/JCLI-D-16-0115.1.
Wu, Z. W., J. P. Li, Z. H. Jiang, and J. H. He, 2011b: Predictable climate dynamics of abnormal East Asian winter monsoon: Once-in-a-century snowstorms in 2007/2008 winter. *Climate Dyn.*, **37**, 1661–1669, https://doi.org/10.1007/s00382-010-0938-4.
Yamaguchi, J., Y. Kanno, G. X. Chen, and T. Iwasaki, 2019: Cold air mass analysis of the record-breaking cold surge event over east Asia in January 2016. *J. Meteor. Soc. Japan*, **97**, 275–293, https://doi.org/10.2151/JMSJ.2019-015.
Yu, Y. Y., M. Cai, C. H. Shi, and R. C. Ren, 2018: On the linkage among strong stratospheric mass circulation, stratospheric sudden warming, and cold weather events. *Mon. Wea. Rev.*, **146**(9), 2717–2739, https://doi.org/10.1175/MWR-D-18-0110.1.
Zhang, P. F., Y. T. Wu, I. R. Simpson, K. L. Smith, X. D. Zhang, B. De, and P. Callaghan, 2018: A stratospheric pathway linking a colder Siberia to Barents-Kara Sea sea ice loss. *Science Advances*, **4**(7), eaat6025, https://doi.org/10.1126/SCIADV.AAT6025.
Zhang, P., Z. W. Wu, and J. P. Li, 2019a: Reexamining the relationship of La Niña and the East Asian winter monsoon. *Climate Dyn.*, **53**, 779–791, https://doi.org/10.1007/s00382-019-04613-7.
Zhang, R. N., C. H. Sun, R. H. Zhang, W. J. Li, and J. Q. Zuo, 2019b: Role of Eurasian snow cover in linking winter - spring Eurasian coldness to the autumn Arctic sea ice retreat. *J. Geophys. Res.*, **124**(16), 9205–9221, https://doi.org/10.1029/2019JD030339.